Assessment of the horizontal resolution of retrieval products derived from MIPAS observations

M. Carlotti[1*], B. M. Dinelli[2], E. Papandrea[1], and M. Ridolfi[1]

[1]*Dipartimento di Chimica Fisica e Inorganica, University of Bologna, Viale Risorgimento 4, 40136 Bologna, Italy*
[2]*Istituto di Scienze dell' Atmosfera e del Clima, CNR, Via P. Gobetti 101, 40129 Bologna, Italy*
[*]*Corresponding author: carlotti@fci.unibo.it*

Abstract: We report the results of a study aimed at the assessment of the trade-off between precision and horizontal resolution of the retrieval products of MIPAS (Michelson Interferometer for Passive Atmospheric Sounding) operating onboard the ENVIronmental SATellite. By exploiting different observation setups we could perform the study by acting on both the retrieval and the sampling grids. Our results are compared with those previously obtained on simulated observations [Appl. Opt. **43**, 1–11 (2004)]. We show that the horizontal sampling of the atmosphere operated by the spectrometer cannot be pushed beyond some limits without inducing unacceptable correlations among the retrieved profiles. These correlations show-up only when using a two-dimensional retrieval algorithm and can be evaluated through the instabilities that they trigger in the horizontal distribution of the retrieval products. In order to reduce these instabilities we compare the strategy of degrading the retrieval grid with the strategy of applying horizontal regularization. We discuss the different trade-off between precision and spatial resolution connected with the two strategies. The method adopted in this study, is applicable to any orbiting limb sounder measuring along the orbit track.

OCIS codes: (0101280) Atmospheric composition; (0101290) Atmospheric optics; (2800280) Remote sensing.

References and links

1. J. W. Waters, W.G. Read, L. Froidevaux, R.F. Jarnot, R.E. Cofield, D.A. Flower, G.K. Lau, H.M. Pickett, M.L. Santee, D.L. Wu, M.A. Boyles, J.R. Burke, R.R. Lay, M.S. Loo, N.J. Livesey, T.A. Lungu, G.L. Manney, L.L. Nakamura, V.S. Perun, B.P. Ridenoure, Z. Shippony, P.H. Siegel, R.P. Thurstans, R.S. Harwood, H.C. Pumphrey, and M.J. Filipiak, "The UARS and EOS Microwave Limb Sounder Experiments," J. Atmos. Sci. **56**, 194-218 (1999).
2. European Space Agency, "Envisat, MIPAS: an instrument for atmospheric chemistry and climate research," SP-1229 (European Space Reseach and Technology Centre, Noordwijk, The Netherlands, 2000).
3. M. J. Endmann, G. Lange and B. Fladt, in *Space Optics 1994: Earth Observation and Astronomy*, M. G. Cerutti-Maori and P. Roussel, eds., Proc. SPIE **2209**, 36 (1994).
4. R. Beer and T. A. Glavich, in *Advanced Optical Instrumentation for Remote Sensing of the Earth's Surface from Space*, G. Duchossois, F. L. Herr and R. J. Zander, eds., Proc. SPIE **1129**, 42 (1989).
5. B. J. Kerridge, J. Barnett, M. Birk, S Buehler, A-C Vandaele, M Carlotti et al., "Process Exploration through Measurements of Infrared and millimetre-wave Emitted Radiation (PREMIER)," Proposal for ESA Core Explorer Mission: CCLRC, SSTD, SSTD-RSG.
6. M. Carlotti, "Global-Fit Approach to the Analysis of Limb-scanning Atmospheric Measurements," Appl. Opt. **27**, 3250-3254 (1988).
7. M. Carlotti, B. Carli, "Approach to the Design and Data-Analysis of a Limb-Scanning Experiment," Appl. Opt. **33**, 3237-3249 (1994)

#81887 - $15.00 USD Received 6 Apr 2007; revised 10 Jul 2007; accepted 19 Jul 2007; published 3 Aug 2007

8. S. Ceccherini, C. Belotti, B. Carli, P. Raspollini and M. Ridolfi, "Technical note: Regularization performances with the error consistency method in the case of retrieved atmospheric profiles," Atmos. Chem. Phys **7**, 1435-1440, (2007).
9. N. J. Livesey and W. G. Read, "Direct retrieval of Line-of-Sight Atmospheric Structure from Limb Sounding Observations," Geophys. Res. Lett. **27**, 891-894 (2000).
10. M. Carlotti, B.M. Dinelli, P. Raspollini, and M. Ridolfi, "Geo-fit Approach to the analysis of limb-scanning satellite measurements," Appl. Opt. **40**, 1872-1885 (2001).
11. J. R. Warden, K. W. Bowman, and D. B. Jones, "Two-dimensional characterization of atmospheric profile retrievals from limb sounding observations," J. Quant. Spectrosc. Radiat. Transfer **86**, 45-71 (2004).
12. T. Steck, M. Hopfner, T. v. Clarmann, U. Grabowski, "Tomographic retrieval of atmospheric parameters from infrared limb emission observations," Appl. Opt. **44**, 3291-301 (2005).
13. M. Ridolfi, L. Magnani, M. Carlotti, B.M. Dinelli, "MIPAS-ENVISAT limb-sounding measurements: trade-off study for improvement of horizontal resolution," Appl. Opt. **43**, 1-11 (2004).
14. M. Ridolfi, B. Carli, M. Carlotti, T. von Clarmann, B.M. Dinelli, A. Dudhia, J.-M. Flaud, M. Hoepfner, P.E. Morris, P. Raspollini, G. Stiller, and R.J. Wells, "Optimized forward model and retrieval scheme for MIPAS near-real-time data processing," Appl. Opt. **39**, 1323-1340 (2000).
15. M. Carlotti, G. Brizzi, E. Papandrea, M. Prevedelli, M. Ridolfi, B.M. Dinelli and L. Magnani, "GMTR: two-dimensional multi-target retrieval model for MIPAS/ENVISAT observations," Appl. Opt. **45**, 716-727 (2006).
16. A. Tikhonov, "On the solution of incorrectly stated problems and a method 5 of regularization," Dokl. Acad. Nauk SSSR **151**, 501-504 (1963).
17. T. Steck, "Methods for determining regularization for atmospheric retrieval problems," Appl. Opt. **41,** 1788-1797 (2002).
18. C. D. Rodgers, Inverse Methods for Atmospheric Sounding: Theory and Practice, Series on Atmospheric, Oceanic and Planetary Physics – Vol. 2 (World Scientific, Singapore, 2000).
19. D. W. Marquardt, "An algorithm for the least-squares estimation of nonlinear parameters," SIAM J. Appl. Math. **11**, 431-441 (1963).
20. P. R. Bevington, D. K. Robinson, Data Reduction and Error Analysis for the Physical Sciences, 3rd edition (McGraw-Hill Higher Education, 2003).
21. T. Steck and T. v. Clarmann, "Constrained profile retrieval applied to the observation mode of the Michelson Interferometer for Passive Atmospheric Sounding," Appl. Opt. **40**, 3559-3571 (2001).
22. A. Dudhia, V. L. Jay, and C. D. Rodgers, "Microwindow selection for high-spectral-resolution sounders," Appl. Opt. **41,** 3665-3673 (2002).
23. J. J. Remedios, "Extreme Atmospheric Constituent Profiles for MIPAS," in *Proceedings of the European symposium on atmospheric measurements from space*, ed.(ESA publication division, 1999), pp 779-783.
24. A. Doicu, F. Schreier, M. Hess, "Iteratively regularized Gauss-Newton method for atmospheric remote sensing," Comp. Phys. Commun. **148**, 214-226 (2002).
25. S. Ceccherini, C. Belotti, B. Carli, P. Raspollini, M. Ridolfi, "Technical Note: Regularization performances with the error consistency method in the case of retrieved atmospheric profiles," Atmos. Chem. Phys. **7**, 1435-1440 (2007).

1. Introduction

Limb-sounding measurements are widely used to collect data on the geographical distribution of atmospheric constituents. Space-borne instruments are quite suited for this observational strategy especially when they measure the atmospheric emission from a polar orbit that allows a full geographical coverage. In these experiments the line of sight of the spectrometer is often oriented along the orbit track. A significant number of this kind of measurements has been realized in the past (e.g. MLS [1], MIPAS [2,3], TES [4]) while others are considered by space agencies for the coming years (e.g. PREMIER [5]). In these experiments, a feature pursued when defining the observation parameters is the optimal spatial-sampling of the atmosphere. In the vertical domain the choice of the sampling grid is driven by the characteristics of the instrument (i.e. the finite Field Of View (FOV)) while, in the horizontal domain, it is determined by the frequency of repetition of the limb scans which, in turn, is connected with the time spent in the vertical sampling (due to the motion of the orbiting platform). In principle, the choice of the observation strategy that determines the sampling of the atmosphere should be operated also considering the retrieval stage; indeed the atmospheric sampling grid should be as much as possible consistent with the capability of the retrieval system to extract information from the observations. If the atmospheric sampling is

#81887 - $15.00 USD Received 6 Apr 2007; revised 10 Jul 2007; accepted 19 Jul 2007; published 3 Aug 2007

exceedingly dense, the sounding of partially overlapping air masses will have to be handled by the retrieval process in order to avoid unphysical oscillations and poor precision of the retrieval products. On the other hand, if the atmospheric sampling leads to a retrieval precision far better than the actual achievable systematic error, it means that a finer atmospheric sampling could have been operated at the observation stage. Of course, the assessment of the consistency between atmospheric sampling and information content of the observations depends on the features of the retrieval algorithm. In the vertical domain the Global-Fit algorithm [6] is suitable to assess the trade-off between spatial resolution and retrieval precision (see e.g. Ref. 7) because it simultaneously retrieves the parameters that define an altitude profile by analyzing a set of observations that contribute to determine it. In the horizontal domain, a two-dimensional algorithm is necessary in order to simultaneously retrieve a set of adjacent altitude profiles by analyzing all the observations that contribute to determine them.

In this paper we deal with the MIPAS experiment and with the assessment of the horizontal resolution of its retrieval products. At the time the experiment was designed, consolidated tools were not yet available to evaluate the consistency between atmospheric sampling step and spatial resolution of the retrieval products. The choice of the vertical sampling was mainly driven by the amplitude of the FOV of the instrument (about 3 km) while the horizontal sampling resulted from the combination of the satellite's horizontal motion with the time spent in measuring a limb sequence. Nowadays, the vertical resolution of the retrieval products obtained with these observational choices is rather well assessed by the wide stream of data analyzed so far; it has been verified that, when the vertical sampling of the atmosphere is finer than the FOV of the instrument, a vertical resolution that matches the sampling step cannot be achieved in the retrieved profiles [8]. In these cases it is necessary either to degrade the retrieval grid or to apply some external constraint (such as the regularization).

The recent advent of two-dimensional retrieval algorithms [9,10,11,12] makes possible the assessment of the spatial resolution also in the horizontal domain; studies have been made in this direction on simulated observations [11,13,12]. In the case of MIPAS, simulated observations have been analyzed in order to establish the trade-off between retrieval precision and horizontal resolution [13]; these analyses were carried out with a prototype retrieval system and adopting several simplifications. In this paper we report the results of a trade-off study based on real MIPAS observations; the analyses were carried out with an operational retrieval system and avoiding most of the simplifications of the previous study. The present work has been extended to all the main retrieval targets of the MIPAS experiment; however in this paper we focus the presentation on the ozone retrievals for which we compare the results with those obtained with simulated observations. Furthermore, we consider the unphysical oscillations that derive from the correlations induced by a too fine horizontal retrieval grid and we compare the performance of two strategies that lead to a smooth distribution of the retrieval products: 1) degradation of the retrieval grid, 2) horizontal regularization of the retrieved field. We show how the trade-off between precision and spatial resolution is affected by the two strategies.

In Sect. 2 we report the features of the MIPAS experiment relevant for this study while in Sect. 3 we recall the basic rationale of the two-dimensional retrieval system used for this study. The mathematical formalism that is functional to the understanding of the results reported in this paper is recalled in Sect. 4. Section 5 is dedicated to describe the trade-off tests and to show their results; the results obtained with real observations are compared in this section with those (when available) that were previously obtained with simulated observations. In Sect. 6 we test and discuss the strategies to damp the horizontal oscillations in the retrieved fields. Finally, in Sect. 7 we draw conclusions and focus on the main findings of the study.

#81887 - $15.00 USD Received 6 Apr 2007; revised 10 Jul 2007; accepted 19 Jul 2007; published 3 Aug 2007

2. The MIPAS experiment

MIPAS (Michelson Interferometer for Passive Atmospheric Sounding) has been developed by the European Space Agency (ESA) for the study of atmospheric composition. MIPAS operates onboard the ENVISAT satellite placed on a nearly polar orbit since March 1st, 2002. The maximum optical path difference of the interferometer is 20 cm that corresponds to a spectral resolution of 0.025 cm^{-1} FT and 0.035 cm^{-1} FWHM unapodized. MIPAS measures the emission of the atmosphere, in the spectral interval from 680 cm^{-1} to 2410 cm^{-1}, with the limb-scanning observation technique. During most of its measuring time, from July 2002 up to March 2004, MIPAS has been operated in the so called "nominal" observation mode that is with consecutive backward-looking limb scans with the line of sight approximately lying in the orbit plane. Each limb scan consisted of 17 observation geometries with tangent altitudes ranging from 6 to 68 km with steps of 3 or 5 km. In the nominal mode the spectral resolution of the instrument was set to its maximum value, implying an horizontal separation between consecutive limb-sequences of about 510 km.

For the study of specific events or atmospheric phenomena MIPAS has also been operated in the so called "special" observation modes. Depending on the scientific objective, the special observation modes may differ from the nominal mode in the adopted spectral resolution, the altitude coverage, the vertical sampling steps, and the azimuth direction of the line of sight. The combination of these observation parameters determines the horizontal spacing between the limb scans of each special mode. In this paper we will consider observations relative to the nominal mode and to the special mode conventionally denoted as S6. The S6 observation mode was designed for measurements in the Upper Troposphere/Lower Stratosphere region with backward-looking limb scans of 12 observation geometries. The tangent altitudes range from 6 to 35 km with 10 steps of 2 km (from 6 to 24 km) and 2 steps at 28 and 35 km. In the S6 mode the spectral resolution of the instrument is reduced to 0.1 cm^{-1} FT. With these observational parameters consecutive limb scans of the S6 mode are horizontally separated by about 155 km.

Due to the deterioration of the interferometric slides, starting from January 2005 all MIPAS observation modes have been re-defined for a "new" configuration in which the instrument is operated at 41% of its maximum spectral resolution. The nominal mode of the new configuration consists of 27 observation geometries whose tangent altitudes range from 6 to 70 km with increasing steps of 1.5, 2, 3, and 4 km. The shorter time required to measure an observation geometry in the new configuration is not fully compensated by the increased number of observation geometries in a limb scan; this leads to a separation of about 410 km between consecutive limb scans.

In the transition phase (from the "old" to the "new" configuration) a set of measurements were performed where the vertical sampling was kept as in the "old" nominal mode while the spectral resolution, and therefore the time required by a limb scan, was reduced. This led to measurements, along a set of orbits, where the horizontal distance between consecutive limb scans is about 260 km.

MIPAS spectra are analyzed by the ESA ground processor that determines, at the tangent points of each limb scan, the values of pressure, temperature and volume mixing ratio (VMR) of six key species (H_2O, O_3, HNO_3, CH_4, N_2O and NO_2). The ground processor uses a retrieval algorithm [14] based on the Global-Fit approach [6]. In this algorithm the portion of atmosphere sounded by the line of sight of the instrument is assumed horizontally homogeneous and observations of a full limb scan are simultaneously processed in order to determine the vertical distribution of the analyzed target. With this strategy a one-to-one correspondence exists between the measured limb scans and the retrieved profiles. The latter are naturally associated with the average geographical coordinates of the tangent points of the corresponding limb scan. Hence, the geophysical parameters retrieved by the Global-Fit (unconstrained) have a spatial separation that is:

#81887 - $15.00 USD Received 6 Apr 2007; revised 10 Jul 2007; accepted 19 Jul 2007; published 3 Aug 2007

a) in the altitude domain; the separation between tangent points,
b) in the horizontal domain; the separation between subsequent limb scans.

3. Rationale of the assessment study

For this study we have used an upgraded version of the open source GMTR code [15]. The main features of GMTR are that it implements the Geo-fit algorithm (described in Ref. 10) and permits the simultaneous retrieval of several targets. We recall that the Geo-fit approach is based on the simultaneous inversion of observations selected from all the limb scans measured along a whole orbit; this strategy makes it possible to model the horizontal variability of the atmosphere. In the Geo-fit the two-dimensional retrieval grid is fully independent from the measurement grid (that is the grid identified by the tangent points of the measurements); by exploiting this feature the atmospheric profiles can be retrieved with horizontal separations that are different from those of the measured limb scans. Therefore, the analysis of the trade-off between horizontal resolution and precision of the retrieval products permits to identify the optimal values of horizontal resolution for a given observation scenario. As for the theoretical study previously made on simulated observations [13], a second strategy has been considered to change the horizontal resolution of the retrieval products; it is based on the possibility to increase the atmospheric sampling by reducing the spectral resolution of the interferometer and therefore the measurement time required by each limb scan. With the simulated observations the trade-off curve was obtained for ozone by acting on the spectral resolution of the MIPAS spectrometer; however the simplification was made to analyze the same spectral features as for the full resolution case. For this purpose the analyzed spectral intervals were widened by a factor equal to the degradation of the spectral resolution but the effect of new transitions, possibly included while widening the spectral intervals, was neglected.

The strategy based on spectral resolution could be tested to some extent with real observations using the MIPAS measurements operated with the "new" measurement scenario.

Irrespective of the adopted strategy, the trade-off between precision and spatial resolution can be tuned with the aim to achieve some precision requirements on the retrieval products. However, when a too fine resolution is asked, the inversion becomes ill-conditioned and the retrieved field is characterized by poor precision and unphysical oscillations. In these cases the option of applying a regularization constraint (see e.g. Refs. 16, 17 and references therein) can be used as an alternative to the degradation of the retrieval grid. In this study we will consider the option of regularization as an additional tool to assess the trade-off between precision and horizontal resolution of the MIPAS products.

4. Mathematical tools

4.1 Retrieval algebra

The open source GMTR code has been upgraded with the option of introducing external constraints in the retrieval process. For the purpose the general iterative solution formula [18]:

$$\Delta\mathbf{x} = \left(\mathbf{x}_{i+1} - \mathbf{x}_i\right) = \left[\mathbf{K}^T\mathbf{S}_n^{-1}\mathbf{K} + \lambda\mathbf{I} + \mathbf{R}\right]^{-1}\left[\mathbf{K}^T\mathbf{S}_n^{-1}\mathbf{n} - \mathbf{R}\left(\mathbf{x}_i - \mathbf{x}_a\right)\right] \qquad (1)$$

has been implemented in order to compute, at iteration i+1, the correction Δx to the state vector x_i. In a GMTR analysis the state vector includes the values of the target quantities at all the geo-located retrieval grid points along the considered orbit. In Eq. (1) **K** is the Jacobian matrix containing the derivatives of the observations analyzed along the full orbit with respect to the elements of the state vector, calculated for $\mathbf{x} = \mathbf{x}_i$. $\mathbf{S}_n$ is the variance-covariance matrix (VCM, assumed non-singular) of vector **n** that contains the differences between each observation and the corresponding simulation, **I** is the identity matrix, λ is the Marquardt damping factor [19], **R** is an operator constraining the solution towards some selected feature

#81887 - $15.00 USD Received 6 Apr 2007; revised 10 Jul 2007; accepted 19 Jul 2007; published 3 Aug 2007

(e.g. value, shape or curvature) of an a-priori state x_a. Typical settings of the **R** matrix are: the inverse of the a priori VCM in the case of optimal estimation [18], or a first or second order discrete derivative operator [16].

Equation (1) is the iterative solution minimizing the χ^2 (cost) function defined as:

$$\chi^2 = \mathbf{n}^{\mathbf{T}}\mathbf{S}_n^{-1}\mathbf{n} + \left(\mathbf{x}_a - \mathbf{x}\right)^T \mathbf{R}\left(\mathbf{x}_a - \mathbf{x}\right). \tag{2}$$

The errors associated with the solution of the inversion procedure are characterized by the VCM of $\Delta\mathbf{x}$ given by:

$$\mathbf{V}_{\Delta x} = \left[\mathbf{K}^T\mathbf{S}_n^{-1}\mathbf{K} + \lambda\mathbf{I} + \mathbf{R}\right]^{-1} \tag{3}$$

The matrix $\mathbf{V}_{\Delta x}$ represents the mapping on the solution of the experimental random error covariance $\mathbf{S}_n$ and of the errors associated with the "pseudo-observations" linked to the applied constraints. The square root of an individual diagonal element of $\mathbf{V}_{\Delta x}$ provides the Estimated Standard Deviation (ESD) of the corresponding retrieved parameter.

For unconstrained retrievals (**R** = **0** and $\lambda = 0$) equations (1), (2), and (3) reduce to the classical Gauss-Newton equations (see e.g. Ref. 15). In this case, if no systematic differences (bias) exist between observed and simulated spectra and if S_n is an adequate estimate of the measurement random error covariance, the quantity χ_R^2 defined as:

$$\chi_R^2 \equiv \frac{\chi^2}{m - p} \tag{4}$$

(where m is the number of observations and p is the number of retrieved parameters) has an expectation value of 1 [20]. Therefore the deviation of χ_R^2 from unity quantifies the capability of the forward model to reproduce the observed spectra and the appropriateness of S_n.

4.2 Definition of spatial resolution

In order to compute the vertical and horizontal resolution of each retrieval parameter the upgraded version of GMTR includes the computation of the averaging kernels matrix [18] as:

$$\mathbf{A} = \left[\mathbf{K}^T\mathbf{S}_n^{-1}\mathbf{K} + \lambda\mathbf{I} + \mathbf{R}\right]^{-1}\mathbf{K}^T\mathbf{S}_n^{-1}\mathbf{K} \tag{5}.$$

In GMTR the retrieval is performed on a two-dimensional grid in which each grid point k is defined by its altitude z_k and its Orbital Coordinate (OC) θ_k., a polar angle originating at the North pole and spanning the orbit plane over its 360° extension. The two-dimensional averaging kernel associated with parameter k is the vector $\boldsymbol{a}(k,j)$, $j=1\ldots p$ (where p is the number of individual grid points) that corresponds to the k^{th} row of matrix **A**. The vertical resolution of a retrieval parameter is defined as the FWHM of the subset of elements of vector $\boldsymbol{a}$ that correspond to the value θ_k of the OC. In a similar way the horizontal resolution is defined as the FWHM of the subset of elements of $\boldsymbol{a}$ that correspond to the altitude z_k.

For unconstrained retrievals **A** reduces to the identity matrix; in these cases the spatial resolution (both vertical and horizontal) of the retrieval parameters coincides with the geometrical separation between the retrieval grid points. Nevertheless, the "intrinsic" spatial resolution of a given set of observations can be determined using the averaging kernel obtained from a regularized retrieval operated with a definitely "dense" retrieval grid.[12].

#81887 - $15.00 USD Received 6 Apr 2007; revised 10 Jul 2007; accepted 19 Jul 2007; published 3 Aug 2007

4.3 Two-Dimensional regularization

In order to introduce a regularization in both the vertical and horizontal domains, matrix **R** of Eq. (5) must be properly defined. In our case matrix **R** is built as the sum of two matrices:

$$\mathbf{R} = \mathbf{S}_a^{-1} + \mathbf{C} \tag{6}$$

where $\mathbf{S}_a$ is a diagonal matrix with entries given by the variances assigned to the elements of the a-priori state x_a. As suggested in Ref. 12, we express **C** as the sum of discrete first-order-derivative matrices, $\mathbf{R}_h$ and $\mathbf{R}_v$, operating a regularization in the horizontal and in the vertical domains respectively:

$$\mathbf{C} = \mathbf{R}_h + \mathbf{R}_v \tag{7}$$

The GMTR analysis system [15] makes the set up of $\mathbf{R}_v$ a simple operation because a common vertical grid is used along the analyzed orbit. Since the retrieval parameters are sequentially arranged in the state vector, vertical profile by vertical profile, matrix $\mathbf{R}_v$ is block-diagonal each block corresponding to a vertical retrieved profile. The structure of $\mathbf{R}_v$ is:

$$\mathbf{R}_v = \begin{matrix} \mathbf{R}_g & 0 & 0 & 0 & 0 \\ 0 & \mathbf{R}_g & 0 & 0 & 0 \\ 0 & 0 & ... & 0 & 0 \\ 0 & 0 & 0 & \mathbf{R}_g & 0 \\ 0 & 0 & 0 & 0 & \mathbf{R}_g \end{matrix} \tag{8}$$

with:

$$\mathbf{R}_g = \frac{1}{\Omega_v^2}\mathbf{L}_v^T\mathbf{L}_v \tag{9}$$

$$\mathbf{L}_v = \begin{matrix} l_1 & -l_2 & 0 & 0 & 0 \\ 0 & l_2 & -l_3 & 0 & 0 \\ 0 & 0 & .. & .. & 0 \\ .. & .. & .. & .. & .. \\ 0 & 0 & 0 & l_{n-1} & -l_n \end{matrix} \tag{10}$$

The matrix element l_k that correlates vertically adjacent parameters is given by:

$$l_k = \frac{1}{\left|z_k - z_{k+1}\right|} \quad . \tag{11}$$

Matrix $\mathbf{R}_h$ of Eq. (7) is assembled with a similar procedure as for $\mathbf{R}_v$; the entries of $\mathbf{R}_h$ are:

$$\mathbf{R}_h = \frac{1}{\Omega_h^2}\mathbf{L}_h^T\mathbf{L}_h \, . \tag{12}$$

In the horizontal domain, parameters that lay on the same altitude level are correlated. Since in GMTR the parameters are sequentially ordered, vertical profile by vertical profile, $\mathbf{L}_h$ is no

#81887 - $15.00 USD Received 6 Apr 2007; revised 10 Jul 2007; accepted 19 Jul 2007; published 3 Aug 2007

longer a block-diagonal matrix as in the vertical domain. The matrix element l_h that correlates horizontally adjacent parameters is computed as:

$$l_h = \frac{1}{\rho_{Earth} \cdot \left| \theta_j - \theta_{j+1} \right|} \tag{13}$$

where θ_j is the OC of the j^{th} profile and ρ_{Earth} is the Earth's radius.

In Eq.s (9) and (12) $\mathbf{\Omega}_v$ and $\mathbf{\Omega}_h$ are input parameters defining the strength of the vertical and horizontal regularization constraints respectively.

5. Trade-off tests

5.1 Trade-off based on the definition of the retrieval grid

In the first set of tests the trade-off was studied by changing the horizontal spacing of the retrieval grid; the retrieval precision was evaluated as a function of the horizontal separation between subsequent retrieved vertical profiles. These tests were performed on a full orbit of observations acquired during the ENVISAT orbit 2081 (from July 24th, 2002); the observations correspond to the nominal mode of the "old" MIPAS configuration. The analyzed frequency intervals are the same as for the theoretical study on simulated observations [13]. The retrievals were carried out without the use of external constraints (**R** = **0** in Eq. (1)). In these tests, since the retrieval grid consists of vertical profiles evenly distributed along the full orbit, the horizontal separation between them (a single scalar quantity) identifies the constant horizontal resolution of the retrieved atmospheric field. Figure 1 refers to ozone and reports a scalar quantifier (ESD quantifier [13]), representing the precision of the retrieved VMRs, as a function of the horizontal resolution. The ESD quantifier is defined as the average of the retrieval ESDs calculated over all the retrieval grid points along the full orbit. In Fig. 1 the trade-off curve obtained analyzing real observations (solid line) is compared with the corresponding curve (dotted line) obtained with simulated observations [13]. The retrieval grid matching the separation between measured limb scans (denoted as *reference* retrieval grid from now on) is marked with an arrow in Fig. 1 as well as in the figures of this type presented later.

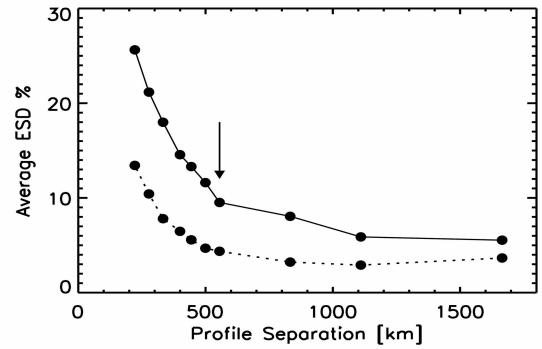

Fig. 1. Trade-off between precision and horizontal resolution for ozone retrievals. The overall precision is represented by the ESD quantifier (see text for definition). The solid and the dotted lines respectively refer to retrievals operated on real and simulated MIPAS observations. The arrow marks the reference retrieval grid of the nominal observation mode.

It can be noticed in Fig. 1 that the trade-off curve obtained with real observations is offset at higher values with respect to the curve obtained with simulated observations. This is a consequence of both the noise of real measurements (which is larger than the nominal values

#81887 - $15.00 USD Received 6 Apr 2007; revised 10 Jul 2007; accepted 19 Jul 2007; published 3 Aug 2007

used in the theoretical study) and the saturation effects introduced by the real atmospheric continuum (which is larger than the model continuum used for the simulated observations). The solid curve in Fig. 1 confirms that, around the value corresponding to the *reference* retrieval grid, the ESD does not change as rapidly as it could be expected with increasing the horizontal resolution [7]. This indicates that the sensitivity of the selected MIPAS measurements to the horizontal variability of the atmosphere encountered along the line of sight, is significant and offers the possibility of increasing the horizontal resolution by paying a relatively low cost in terms of retrieval precision. In particular, Fig. 1 suggests that the horizontal resolution can be doubled with respect to the reference retrieval grid, at the cost of an increment of a factor slightly larger than 2 in the average ESD.

Figure 2 shows the behavior of χ_R^2 (see Eq. (4)) for the retrievals reported in Fig. 1. Again, in Fig. 2 the solid line refers to the values obtained analyzing real observations while the dotted line reports the values obtained with simulated observations [13]. As expected, in the case of real observations the values of χ_R^2 are higher than the corresponding ones for simulated observations where no systematic errors affect the residuals of the fitting procedure.

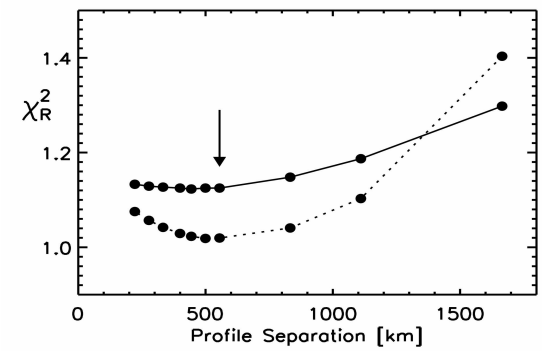

Fig. 2. Variation of χ_R^2 as a function of the horizontal resolution for the retrievals reported in figure 1. The drawing notations are the same of fig. 1.

About Fig. 2 we notice that:

In the case of simulated observations the minimum value of χ_R^2 corresponding to the reference retrieval grid is due to the fact that the horizontal step of this grid roughly matches the horizontal resolution of the atmospheric model used to generate the synthetic observations. For retrieval grids coarser than the reference grid the χ_R^2 increases because the forward model is no longer able to capture the horizontal variability of the atmosphere and therefore to properly fit the observations. For retrieval grids finer than the reference grid χ_R^2 increases as well, because the redundancy of the retrieval grid is not useful to reduce the residuals of the fit (the horizontal variability of the atmosphere is properly modeled by the reference retrieval grid) while it significantly decreases the denominator of Eq. (4).

In the case of real observations the behavior of χ_R^2 is similar to the previous case for grids that are equal to or coarser than the reference grid. For grids that are finer than the reference grid χ_R^2 remains almost constant indicating that the benefit deriving from the increasing number of degrees of freedom (that enables a better modeling of the horizontal structures of the atmosphere) prevails on the decrease of the denominator of Eq. (4).

Figure 3 reports the ESD trade-off curve for ozone (green line already shown in Fig. 1) together with the analogous curves obtained for the retrieval of pressure (orange), temperature (red) and water (blue). Figure 3 confirms, for all these targets, the indication obtained for the

#81887 - $15.00 USD Received 6 Apr 2007; revised 10 Jul 2007; accepted 19 Jul 2007; published 3 Aug 2007

ozone retrieval that is: a factor of two improvement in the horizontal resolution leads to a factor between two and three of degradation for the ESD of the retrieved profiles.

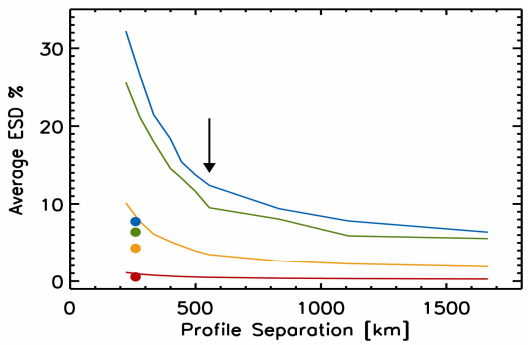

Fig. 3. Trade-off curves for the retrieval of pressure (orange), temperature (red), water (blue) and ozone (green, already shown in figure 1). The value of the ESD quantifiers is also reported (with the same colors) for the retrievals operated on reduced resolution measurements.

5.2 Trade-off based on spectral resolution

The transition period between the "old" and the “new” MIPAS configurations (see Sect. 2) gave the opportunity to operate a test in which the reference retrieval grid is made more dense by the reduction of spectral resolution. The “new” MIPAS nominal observation mode could not be used to perform this test since, as reported in Sect. 2, the altitude steps of the limb scans are so different from those of the old configuration that the different correlations in the vertical domain prevent any estimate of the effects due to the variation in the horizontal sampling of the atmosphere. However, as discussed in Sect. 2, the observation geometries of the “old” nominal mode were retained for the limb scans operated for a few days in August 2004. Therefore we have used the reference retrieval grid of this temporary observation mode in the analysis of both the new orbits and of orbit 2081. For the purpose of this test we have selected optimal spectral intervals for the analysis of the reduced spectral resolution observations [22]. The precision of the retrieval products obtained in the two cases is expected to provide indications about the performance of the two strategies. A comparison is shown in the maps of Fig. 4 reporting the geographical distributions of the ESD associated with the retrieved ozone VMR. Panel (a) of Fig. 4 refers to orbit 12858 (recorded in August 2004) while panel (b) refers to orbit 2081. In Fig. 4, as well as in Fig. 6 (see Sect. 6), the white bands correspond to regions of the atmosphere in which the presence of clouds invalidates the observations. The value of the ESD quantifier corresponding to panel (a) of Fig. 4 is reported in Fig. 3 (full symbols) together with the quantifiers obtained from orbit 12858 for all the targets considered in this figure. These tests were performed using $\mathbf{R} = \mathbf{0}$ in the iterative formula of Eq. (1).

#81887 - $15.00 USD Received 6 Apr 2007; revised 10 Jul 2007; accepted 19 Jul 2007; published 3 Aug 2007

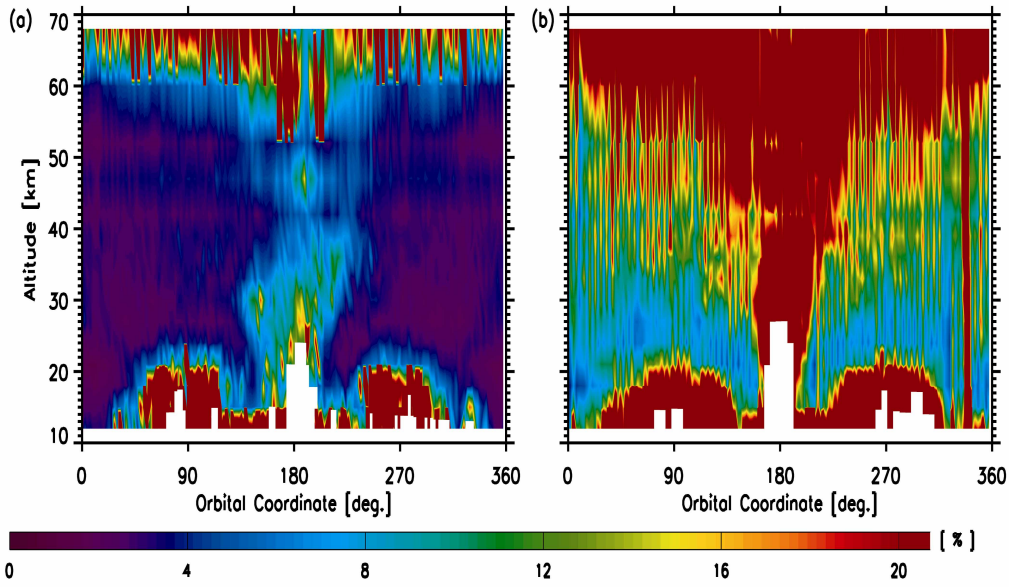

Fig. 4. Percent value of the ESDs associated with the retrieved ozone VMRs. Panel (a) refers to reduced spectral resolution measurements, panel (b) refers to full spectral resolution measurements. The white bands correspond to regions of the atmosphere in which the presence of clouds invalidates the observations.

5.3 Comparison of the two strategies

For a correct evaluation of the results shown in Figs. 3 and 4 it must be recalled that different observations have been analyzed in the compared retrievals; however the total number of analyzed spectral points is comparable in the two cases. Beyond these considerations, Fig. 4 clearly shows that in order to gain horizontal resolution the strategy based on the reduction of spectral resolution (and then of the measurement time) is advantageous with respect to the strategy of using a finer retrieval grid. The advantage is confirmed in Fig. 3 by the position of the dots relative to the four targets; in all cases the ESD quantifier of the reduced spectral resolution lies below the value in the corresponding trade-off curve. This outcome is consistent with the indication reported in Ref. 13 that was obtained with simulated observations and making use of several assumptions.

A conclusive sentence about the merit of the two strategies must include an evaluation of the systematic errors associated with the observations that have been analyzed. In both cases the selection of the observations was carried out with a software, explicitly developed for MIPAS [22], that operates on the basis of the error components associated with the individual spectral points. This software also provides an estimate of the total systematic error at all the retrieval altitudes. Figure 5 refers to ozone and shows, with a solid line, the altitude profile of the percentage total systematic error associated with the set of observations analyzed in the reduced resolution measurements and, with a dashed line, the analogous profile associated with the full resolution measurements. The differences of the two error profiles reported in Fig. 5 are not such to invalidate the advantages on the ESDs obtained with the strategy based on the reduction of spectral resolution.

6. Horizontal smoothing

A prominent feature in panel (b) of Fig. 4 is the fine horizontal oscillations of the ESD values that appear at most altitudes. Although much less pronounced, similar oscillations are also visible in panel (a) of the same figure. This feature also appears in the corresponding maps (not shown) reporting the VMR distributions and becomes more and more evident while the

#81887 - $15.00 USD Received 6 Apr 2007; revised 10 Jul 2007; accepted 19 Jul 2007; published 3 Aug 2007

retrieval grid becomes more and more dense in the trade-off tests described in Sect. 5.1. These oscillations are the result of two concurrent effects:

1. the occasional coincidence of the OC of the retrieved profiles with the OC of the tangent points of the observations (where the information is largest).
2. the negative-correlation between adjacent retrieval grid points at the same altitude that increases when the profiles get closer.

The first effect is expected to minimize the oscillations with the reference retrieval grid (as in the case of panel (a) of Fig. 4) and to maximize them when this grid is doubled (case close to the one shown in panel (b) of Fig. 4). The second effect is further discussed in this Section.

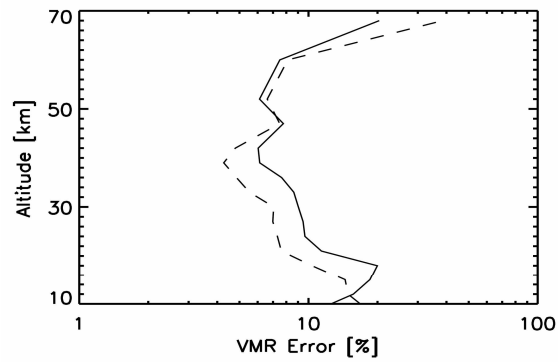

Fig. 5. Altitude distribution of the percentage systematic error associated with the set of observations analyzed in the reduced spectral resolution measurements (solid line) and in the full spectral resolution measurements (dashed line).

In the vertical domain, the extension of the FOV of the spectrometer is usually the parameter driving the choice of the vertical sampling step of limb measurements. In the horizontal domain the choice of the sampling step is not directly connected to a single parameter but, as mentioned in Sect. 1, is instead determined by a combination of several factors. For this reason the effort to collect the maximum amount of information may lead to push the horizontal sampling regardless of the correlations that will affect the retrieval products. A meaningful example of correlation induced by the horizontal over-sampling of the

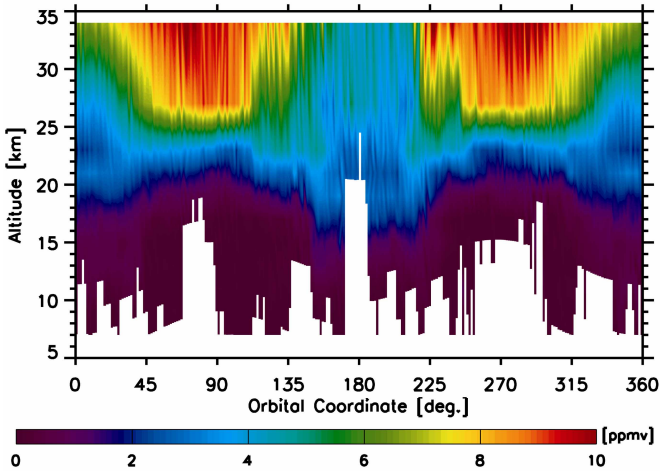

Fig. 6. Ozone VMRs retrieved by GMTR from the measurements of MIPAS with the S6 observation mode. The white bands correspond to regions of the atmosphere in which the presence of clouds invalidates the observations.

#81887 - $15.00 USD Received 6 Apr 2007; revised 10 Jul 2007; accepted 19 Jul 2007; published 3 Aug 2007

atmosphere is provided by the S6 observation mode where the neighboring limb-scans are separated by about 155 km (see Sect. 2). The map in Fig. 6 shows the distribution of the ozone VMR retrieved on the reference retrieval grid by GMTR from the measurements of ENVISAT orbit 7023 in which MIPAS was operated in the S6 observation mode. The horizontal oscillations, visible in Fig. 6, are clearly unphysical and also appear in the corresponding map (not shown) of the ESDs whose values increase by effect of the strong correlations between horizontally adjacent retrieval grid points. This effect is of the same nature of the instabilities that appear in the altitude profiles when the observations have been performed with a vertical over-sampling. The size of the oscillations in Fig. 6 can be better evaluated in Fig. 7 where the blue line shows the ozone VMR values retrieved at 28 km limited (for clarity) to the orbit section going from the North pole to the equator. It is worth to point out that the instabilities induced by the horizontal correlations only appear and can be evaluated by a two-dimensional retrieval algorithm.

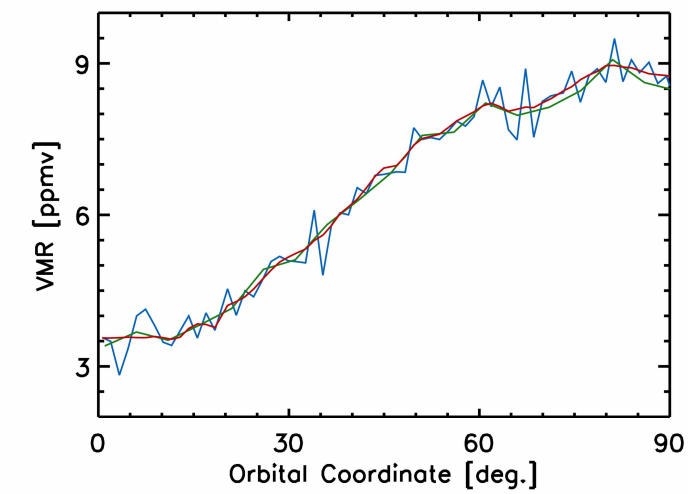

Fig. 7. Ozone VMR values retrieved at 28 km from S6 observation mode measurements. The three curves were obtained using the reference retrieval grid (blue), using a retrieval grid in which the profiles are separated by about 550 km (green), applying regularization in the horizontal domain to the profiles retrieved in correspondence of the reference retrieval grid (red).

As for the vertical profiles, two strategies can be used in order to damp the unphysical oscillations in the horizontal distribution of the retrieved atmospheric parameters: 1) increase the horizontal spacing of the retrieval grid, 2) apply regularization. The issue then becomes the assessment of the advantages and disadvantages of the two strategies. For this purpose we will use the horizontal distribution at 28 km, reported in Fig. 7, that is representative of the general behavior. The retrieval from the S6 observations of orbit 7023 has been repeated using the two strategies mentioned above in order to smooth out the horizontal distribution. Regularization in the horizontal domain was applied to the ozone fields retrieved in correspondence of the reference grid. For the purpose climatological profiles [23] were used as both initial guess and background state ($\mathbf{x}_a$ of Eq. 1) of the retrieval; a regularization strength $\Omega_h = 0.75$ (see Eq. 12) was selected as this value leads to an increase (with respect to the non-regularized case) of χ^2_R (see Eq. 4) which is comparable with the threshold variation of this parameter adopted for the convergence criterion of the iterative procedure. The red line of Fig. 7 shows the ozone distribution resulting from the regularized retrieval; in the same figure the green line shows the distribution obtained by retrieving ozone profiles separated by about 550 km, separation that provides a smooth distribution equivalent to the one obtained

#81887 - $15.00 USD Received 6 Apr 2007; revised 10 Jul 2007; accepted 19 Jul 2007; published 3 Aug 2007

by means of regularization. In order to compare the performance of the two retrieval strategies, Fig. 8 shows the absolute value of the ESDs obtained in the two cases while Fig. 9 shows the corresponding values of the horizontal resolution computed from the **A** matrix (see Sect. 4.2).

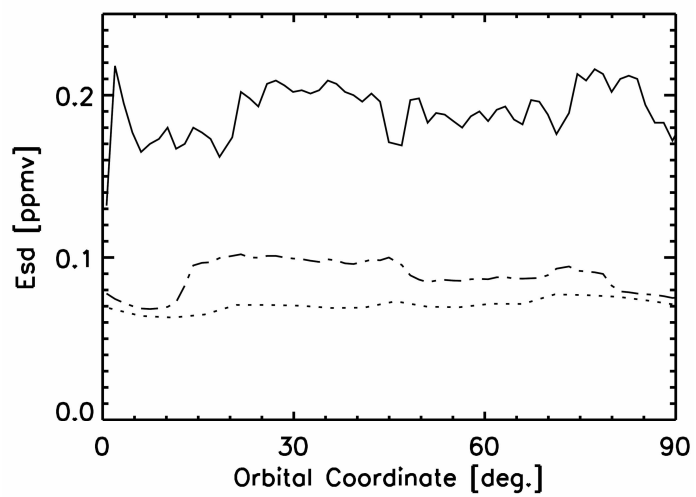

Fig. 8. Absolute value of the ESDs associated with the ozone VMRs reported in Fig. 7. The solid, dotted and dot-dashed lines report respectively the reference, the dispersed-grid, and the regularized cases.

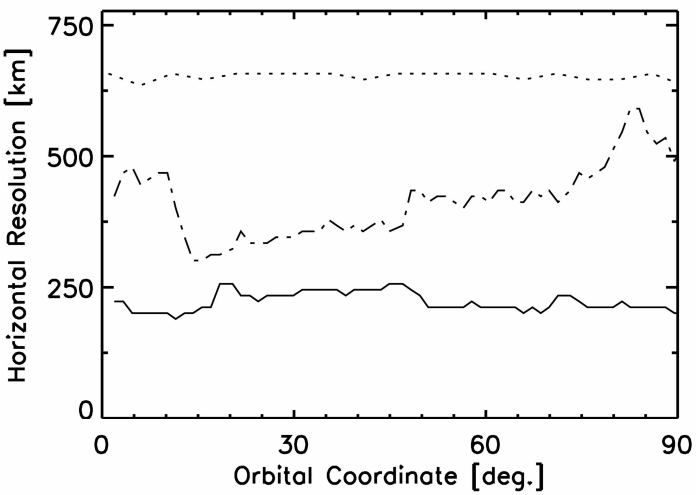

Fig. 9. Value of the horizontal resolution associated with the ozone VMRs reported in Fig. 7. The notations are the same of Fig. 8.

In both Figs. 8 and 9 the solid, dotted, and dot-dashed lines report the reference, the dispersed-grid, and the regularized cases respectively. Figure 9 shows that the horizontal resolution of the reference and dispersed-grid cases is lower than the constant separation between the retrieved profiles (about 155 km and 558 km respectively). This is due to the Marquardt λ that was set = 0.1 in the retrieval formula (see Eq. (1)) as a constant damping factor in all three cases in order to stabilize the retrieval procedure; the λ factor acts as a constraint degrading the horizontal resolution.

#81887 - $15.00 USD Received 6 Apr 2007; revised 10 Jul 2007; accepted 19 Jul 2007; published 3 Aug 2007

Figure 8 shows that the strategy of widening the retrieval grid leads to a rather constant precision of the retrieval products which is slightly better than the one observed with the strategy of regularization. On the other hand, it can be seen in Fig. 9 that the strategy of regularization provides a variable horizontal resolution that is remarkably better than that obtained with the other strategy. Indeed the effectiveness of the regularization depends on the information content of the analyzed observations. The comparison of the dot-dashed lines in Figs. 8 and 9 confirms that the horizontal resolution is negatively-correlated with the ESD along the orbital coordinate.

As a general consideration we notice that the strategy of widening the retrieval grid implies a reduced demand of computing resources with respect to regularization. Furthermore, the strategy of regularization is not a straightforward choice because it is difficult to establish a value of the regularization strength that is of general validity for the different scenarios encountered in routine measurements; several studies have been devoted to this subject (see e.g. Refs. 12, 24, 25). On the other hand, a consequence of the regularization process is that the spatial resolution of the retrieval products does no longer coincide with the distance of the retrieval grid points. Therefore, in the case of regularization, the spatial resolution can be assessed only through the calculation of the averaging kernels. This makes the interpretation of the retrieved geophysical quantities more difficult for users that are not skilled in the retrieval theory.

7. Conclusions

In this paper we report the results of a study aimed at the assessment of the horizontal resolution of level 2 products derived from real MIPAS observations. A two-dimensional retrieval algorithm has been used to determine the trade-off between precision and horizontal resolution of the atmospheric fields of pressure, temperature, water, and ozone. The results related to ozone have been compared with those previously obtained with simulated observations.

Two different strategies have been considered in order to change the horizontal resolution of the retrieval products:

1. Nominal mode measurements were analyzed on a horizontal retrieval grid different from the measurement grid.
2. A finer horizontal sampling of the atmosphere has been obtained at the expenses of the spectral resolution.

The analysis on real measurements with the first strategy confirms that the horizontal resolution of the retrieved profiles can be improved by a factor of two with respect to the value determined by the atmospheric sampling interval. The second strategy has been tested using MIPAS observations acquired with a spectral resolution reduced by a factor of about 60% with respect to its maximum value. The comparison of the two strategies has shown that the second one is more effective in order to improve the horizontal resolution. This confirms the indication that was obtained with simulated observations and making use of several simplifying assumptions [13].

It has been shown that, as in the vertical domain, unphysical horizontal oscillations are triggered by a too fine retrieval grid. These instabilities, that can be evaluated only by a two-dimensional retrieval algorithm, are induced by horizontal correlations. In these cases two strategies have been considered that permit to obtain a smooth distribution of the atmospheric parameters: 1) degradation of the horizontal retrieval grid, 2) regularization. In the considered test cases it was found that the first strategy is advantageous from the point of view of the precision while the second provides a variable but definitely better horizontal resolution of the retrieved products.

The quantitative findings reported in this paper are applicable only to the MIPAS experiment. However, the qualitative conclusions and the used methods can be extended to any satellite limb-scanning instrument measuring the atmosphere along the orbit track.

#81887 - $15.00 USD Received 6 Apr 2007; revised 10 Jul 2007; accepted 19 Jul 2007; published 3 Aug 2007